

Supporting Information

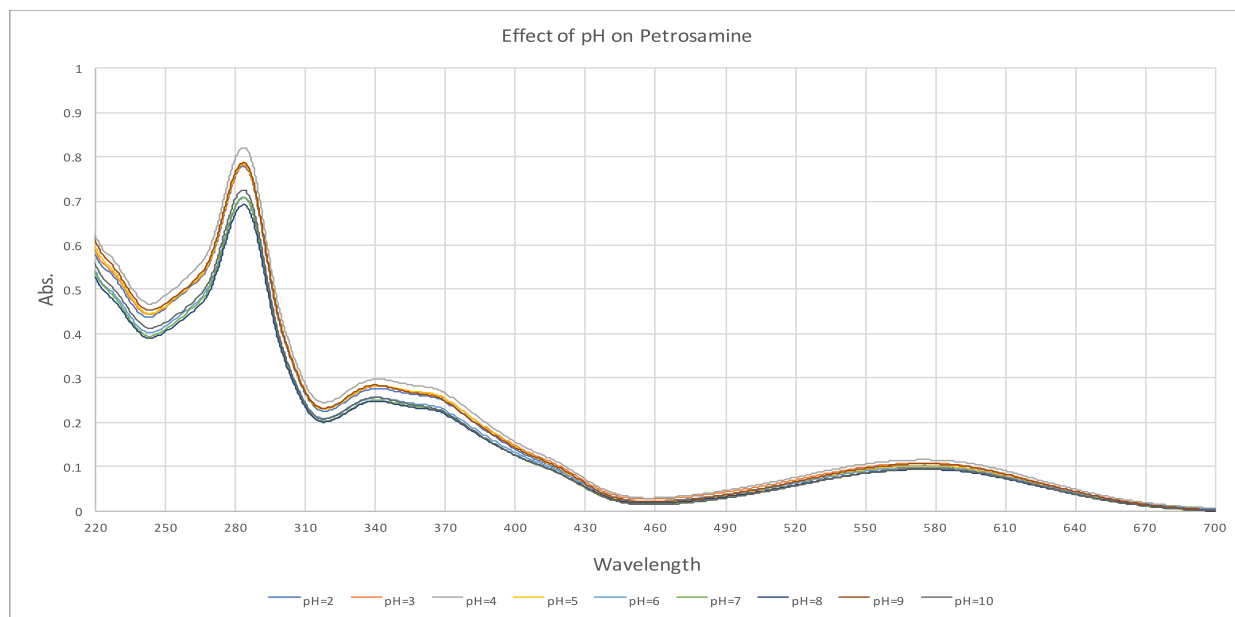
Petrosamine Revisited. Experimental and Computational Investigation of Solvatochromism, Tautomerism and Free Energy Landscapes of a Pyridoacridinium Quaternary Salt.

Christopher Gartshore¹, Yongxuan Su¹ and Tadeusz F. Molinski^{1,2,*}

- 1 Department of Chemistry and Biochemistry, University of California, San Diego, 9500 Gilman Drive, La Jolla, CA 92093, USA MC3568; gartcj@gmail.com
2 Skaggs School of Pharmacy and Pharmaceutical Sciences, University of California, San Diego, 9500 Gilman Drive MC3568, University of California, San Diego, 9500 Gilman Drive, La Jolla, CA 92093, USA.
* Correspondence: tmolinski@ucsd.edu

Page	Title	Content
S1.	Figure S1	UV-vis spectra of 1 . pH dependence in Britton-Robinson buffer (normalized).
S2	Figure S2.	FTIR of 6b (film, ATR)
S2.	Figure S3.	UV-vis spectra of 6b in pure acetone
S3.	Figure S4.	UV-vis spectra of 6b in acetone-H ₂ O mixtures (normalized)
S3.	Table S1.	λ_{\max} and absorbance of merocyanine dye 6b in H ₂ O-acetone mixtures.
S4.	Figure S5.	In situ ESIMS measurements of the rate of H-D exchange of 1 in CD ₃ OD.
S5.	S6	Derivation of kinetic parameters of H-D exchange of 1 in CD ₃ OD and uncertainty analysis.

Figure S1. UV-vis spectra of **1**. pH dependence in in Britton-Robinson buffer¹ (pH 2 – 10, normalized)



¹Britton, H. T. K.; Robinson, R. A. CXCVIII.—Universal buffer solutions and the dissociation constant of veronal. *J. Chem. Soc.* **1931**, 1456-1462.

Figure S2. FTIR spectrum of 6b

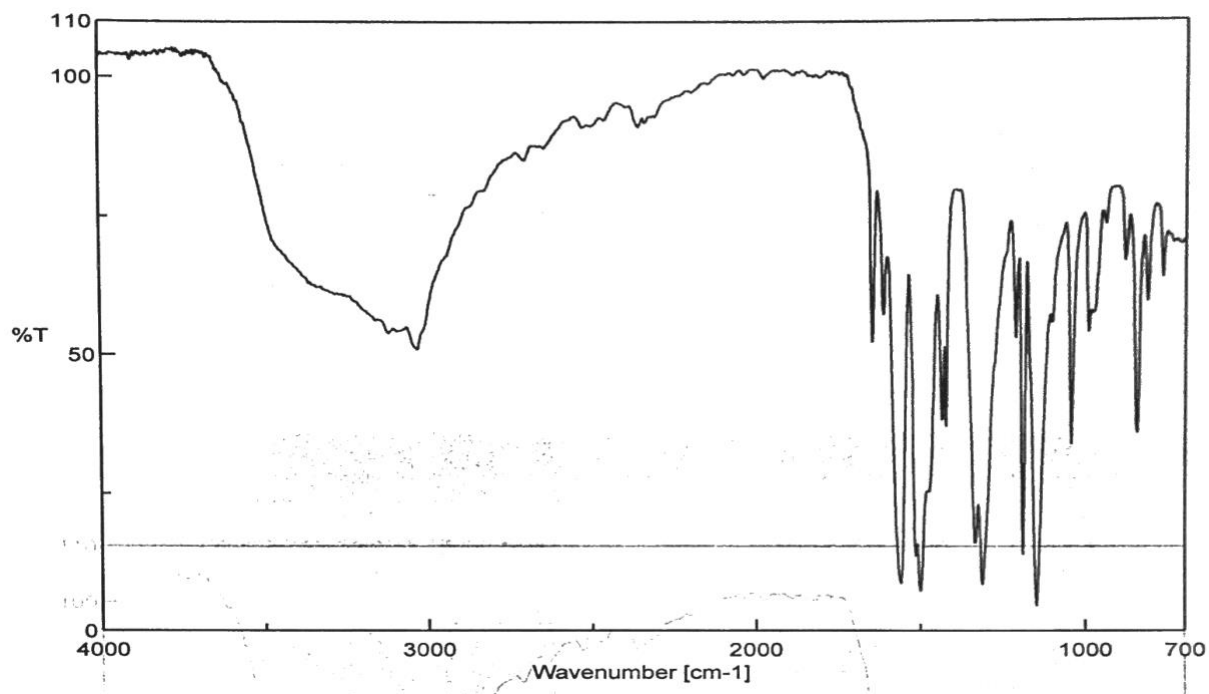


Figure S3. UV-vis spectrum of 6b in acetone (lmax2 = .

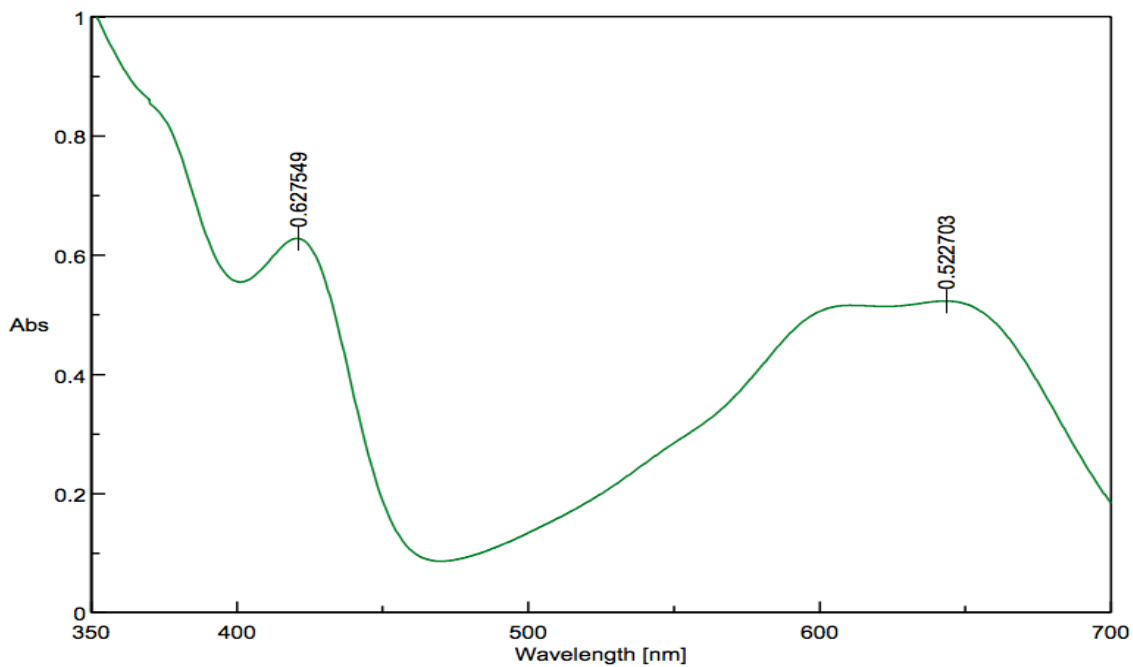
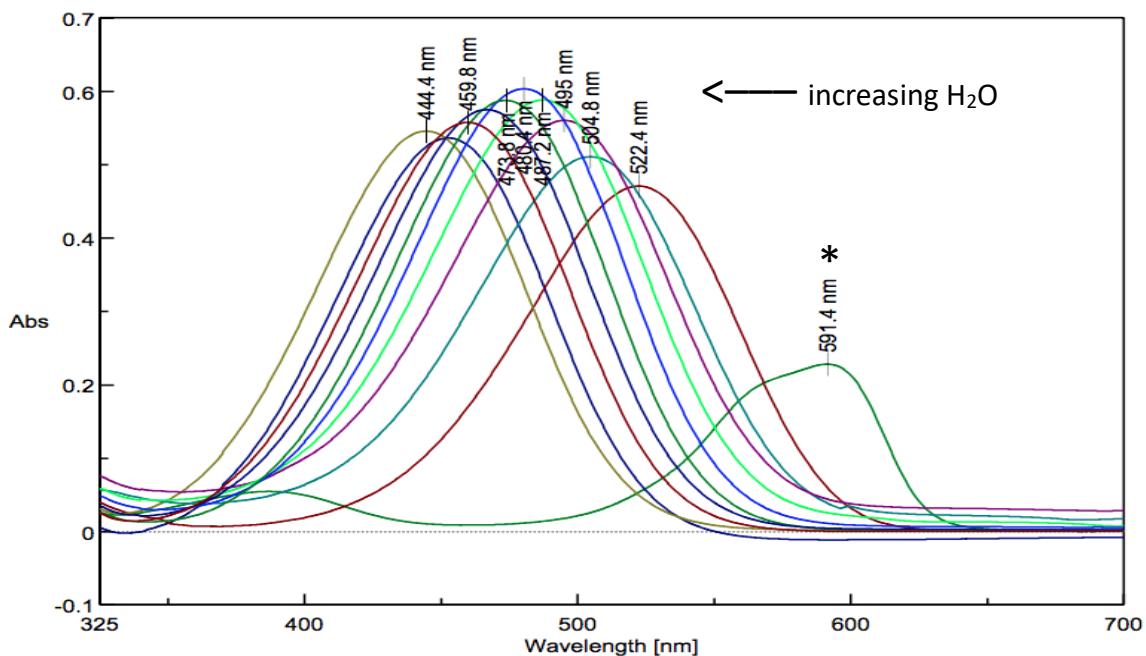


Figure S4. UV-vis spectra of **6b** in acetone-H₂O mixtures¹ (normalized).



¹Each with 5 μ L *n*Bu₄N⁺ HO⁻: 0% H₂O*, 20%, 30%, 40%, 50%, 60%, 70%, 80%, 90% and 100%).

Table S1. λ_{\max} and absorbance of merocyanine dye **6b** in H₂O-acetone mixtures.

%H ₂ O (v/v)	λ_{\max} ¹	Absorbance
0	591.4	0.227779
10	522.4	0.459048
20	504.8	0.510442
30	495.0	0.559982
40	487.2	0.587949
50	480.4	0.603025
60	473.8	0.587191
70	466.8	0.574550
80	459.8	0.557193
90	450.8	0.535364
100	444.4	0.545338

¹See text for definition of 'band-1' and 'band-2'

Figure S5. In situ ESIMS measurements of the rate of H-D exchange of **1** in CD₃OD.¹

¹*t* = 0' values normalized to a solution of **1** CH₃OH

S6. Derivation of kinetic parameters of H-D exchange of petrosamine (1) in CD₃OD and uncertainty analysis.

Petrosamine (1) was dissolved in CD₃OD and aliquots of the solution sampled by ESIMS every 15 s from 15 s to 120 s. Three replicate runs were completed.

Assuming the kinetics of each of the two elemental steps in H-deuterium exchange reaction follow first-order rate laws and that the reverse reactions can be ignored (high concentration of CD₃OD), the following analysis is valid (note: A = 1-d₀, B = 1-d₁ and C = 1-d₂,



The reaction rate of A, B and C could be defined by eq. (1)-(3), and their initial concentrations were shown in eq (4)

$$\left\{ \begin{array}{l} \frac{d[A]}{dt} = -k_1[A] \quad (1) \\ \frac{d[B]}{dt} = k_1[A] - k_2[B] \quad (2) \\ \frac{d[C]}{dt} = k_2[B] \quad (3) \\ [A]_0 = 1, [B]_0 = [C]_0 = 0 \quad (4) \end{array} \right.$$

The solution to the system of the differential equations above were shown in eq (5)-(7) (also see note):

$$[A]_t = e^{-k_1 t} \quad (5)$$

$$[B]_t = \frac{k_1(e^{-k_2 t} - e^{-k_1 t})}{k_1 - k_2} \quad (6)$$

$$[C]_t = \frac{k_2 e^{-k_1 t} - k_1 e^{-k_2 t}}{k_1 - k_2} + 1 \quad (7)$$

k_1 could be obtained by fitting experimental [A] to eq (5) using nonlinear regression or linear regression.

k_2 could be obtained by fitting experimental [B] to eq (6) using nonlinear regression or by fitting experimental [C] to eq (7) using nonlinear regression, using k_1 value obtained from eq (5).

Fitting k_1 and k_2 simultaneously to (6) or (7) was possible, but it generated a large error in k_1 and therefore k_1 was obtained by using eq (5) only.

Only the data in first 45 s of reaction were used for k_1 fitting, and the data in the first 60 s were used for k_2 fitting.

Note:

eq (6) and eq (7) were only valid when $k_1 \neq k_2$. When $k_1 = k_2 = k$, they became:

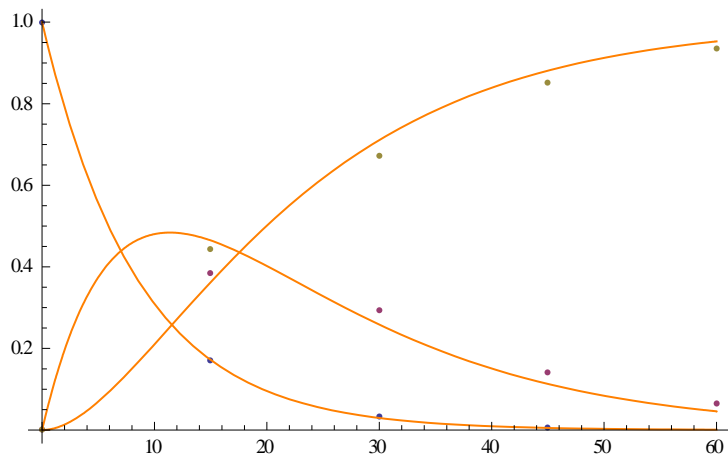
$$[B]_t = kte^{-kt} \quad (8)$$

$$[C]_t = 1 - e^{-kt} - kte^{-kt} \quad (9)$$

It could be demonstrated that eq (6) and (7) converged to (8) and (9) when $k_1 - k_2 \rightarrow 0$ using Taylor expansion.

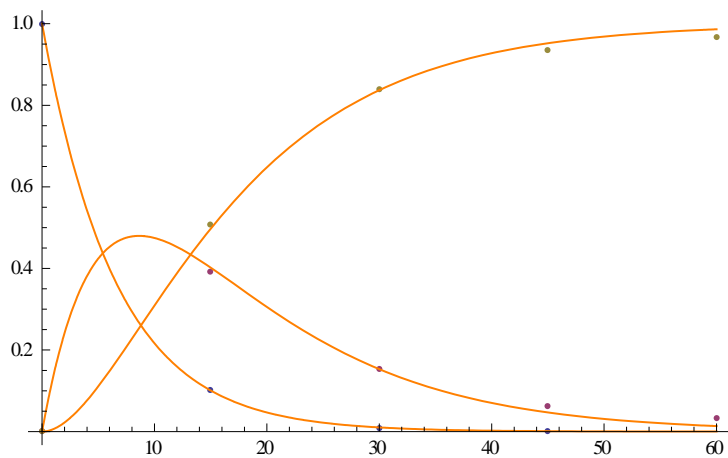
1st Run (Run B):

	k (s^{-1})	Standard Error (σ)	95% Confidence Interval	R^2
k_1 (fitting to eq. 5)	0.1175	0.0009	{0.1147, 0.1203}	0.99998
k_2 (fitting to eq. 6)	0.0638	0.0063	{0.0463, 0.0813}	0.97
k_2 (fitting to eq. 7)	0.0635	0.0064	{0.0456, 0.0814}	0.996



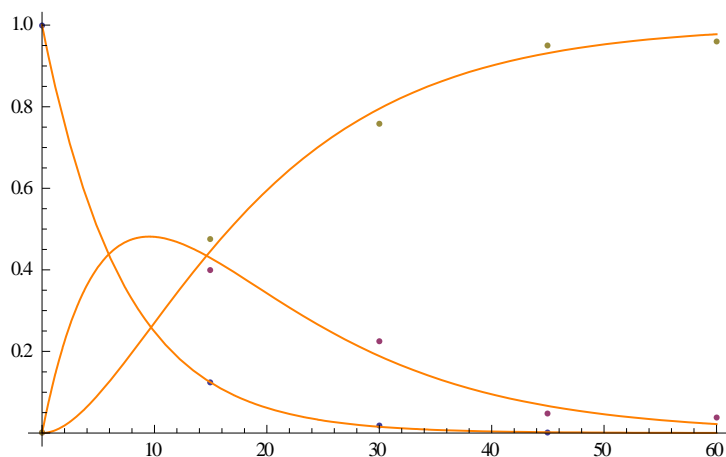
2nd Run (Run C):

	k (s^{-1})	Standard Error (σ)	95% Confidence Interval	R^2
k_1 (fitting to eq. 5)	0.1531	0.0007	{0.1507, 0.1555}	0.999996
k_2 (fitting to eq. 6)	0.0850	0.0028	{0.0772, 0.0927}	0.996
k_2 (fitting to eq. 7)	0.0850	0.0029	{0.0769, 0.0932}	0.9997



3rd Run (Run D):

	k (s^{-1})	Standard Error (σ)	95% Confidence Interval	R^2
k_1 (fitting to eq. 5)	0.1394	0.0007	{0.1371, 0.1417}	0.999994
k_2 (fitting to eq. 6)	0.0767	0.0046	{0.0641, 0.0893}	0.99
k_2 (fitting to eq. 7)	0.0765	0.0047	{0.0634, 0.0896}	0.999



Although k_1 and k_2 showed some variation between runs, it is interesting to observe that $k_2/k_1 = 0.55$ among all three runs.

Summary:

1. Run #1 (B) $k_1 = 0.11750(9) s^{-1}$, $k_2 = 0.0635(64) s^{-1}$ $R^2 = 0.99998$ Eqn. 5
2. Run #2 (C) $k_1 = 0.1531(7) s^{-1}$, $k_2 = 0.0850(29) s^{-1}$ $R^2 = 0.99996$ Eqn. 7
3. Run #3 (D) $k_1 = 0.1394(7) s^{-1}$, $k_2 = 0.0765(47) s^{-1}$ $R^2 = 0.999994$ Eqn. 7